Fédération Internationale du Béton
Proceedings of the 2nd International Congress
June 5-8, 2006 – Naples, Italy

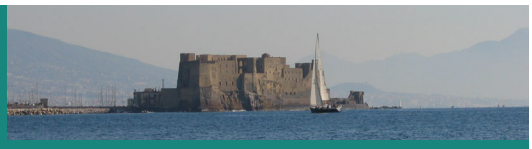

ID 10-86 Session 10 – FRP reinforcement for new and existing structures

The Influence of Service Temperature on Bond between FRP Reinforcement and Concrete

Leone, M., Aiello, M.-A.
Department of Innovation Engineering, University of Lecce, Via per Arnesano, 73100 Lecce, Italy

Matthys, S.
Magnel Laboratory for Concrete Research, Department of Structural Engineering, Ghent University, Technologiepark-Zwijnaarde 904, B-9052 Gent, Belgium

INTRODUCTION

The interest in fibre reinforced polymer (FRP) reinforcement in construction has considerably increased and especially the application of FRP as externally bonded reinforcement (FRP EBR) has become more and more established. The use of FRP EBR has been adopted world-wide as a very attractive technique for structural strengthening and rehabilitation [1]. At Ghent University, the fire behaviour of slabs and beams strengthened with advanced composites, including the use of fire protection systems, has been investigated [2-4]. In addition, the behaviour of the FRP-concrete interface at increased temperatures has been considered [5,6], as elevated temperatures may occur during service conditions, especially for outdoor applications. According to fib Bulletin 14 [7], the glass transition temperature of the adhesive used to bond the FRP should equal 20°C in excess of the maximum ambient temperature at normal service conditions, and should be at least 45°C. When reaching the glass transition temperature, the properties of the adhesive decrease to a large extend and bond interaction between the concrete and the external FRP reinforcement may be completely lost.
To study the bond behaviour at elevated temperatures, a joint test program between the Universities of Ghent and Lecce has been executed, comprising a series of 20 bond tests performed at the Magnel Laboratory for Concrete Research. The present paper will discuss the experimental work and the main test results obtained.

Keywords: concrete, FRP, externally bonded reinforcement, bond, temperature

OUTLINE OF THE EXPERIMENTS

Test specimens and parameters

The experimental program comprises 20 double-face bond shear tests, tested at different temperatures up to 80°C (Table 1). The type of test specimen used to study the bond behaviour at elevated temperatures is illustrated in Fig. 1. The concrete specimen (150x150x800 mm) is formed by two concrete prisms (150x150x400 mm). A thin metal plate separates the two concrete prisms. The height of this plate is at both sides 15 mm less than the height of the prisms, so that both prisms remain aligned during specimen manipulation and application of the FRP. Two steel bars with a diameter of 16 mm are embedded into each prism. These bars do not connect the two concrete prisms, which means that the two prisms are only connected through the surface bonded FRP reinforcement. The length of the protruding part of the steel bars was chosen in order to guarantee the clamping in the tensile testing machine.

Tab. 1. Overview of test specimens

Specimens	FRP reinforcement	Post Cure	Test temperature (°C)	Batch no.
C_S_20_a	CFRP sheet	No	20	I
C_S_20_b	CFRP sheet	No	20	I
C_S_50_a	CFRP sheet	No	50	I
C_S_50_b	CFRP sheet	No	50	II
C_S_65_a	CFRP sheet	No	65	I
C_S_65_b	CFRP sheet	No	65	II
C_S_80_a	CFRP sheet	No	80	I
C_S_80_b	CFRP sheet	No	80	II
C_L_20_a	CFRP laminate	No	20	I
C_L_20_b	CFRP laminate	No	20	II
C_L_50_a	CFRP laminate	No	50	III
C_L_50_b	CFRP laminate	No	50	III
C_L_80_a	CFRP laminate	No	80	II
C_L_80_b	CFRP laminate	No	80	II
C_L_PC_a	CFRP laminate	Yes	20	II
C_L_PC_b	CFRP laminate	Yes	20	II
G_S_20_a	GFRP sheet	No	20	III
G_S_20_b	GFRP sheet	No	20	III
G_S_80_a	GFRP sheet	No	80	III
G_S_80_b	GFRP sheet	No	80	III

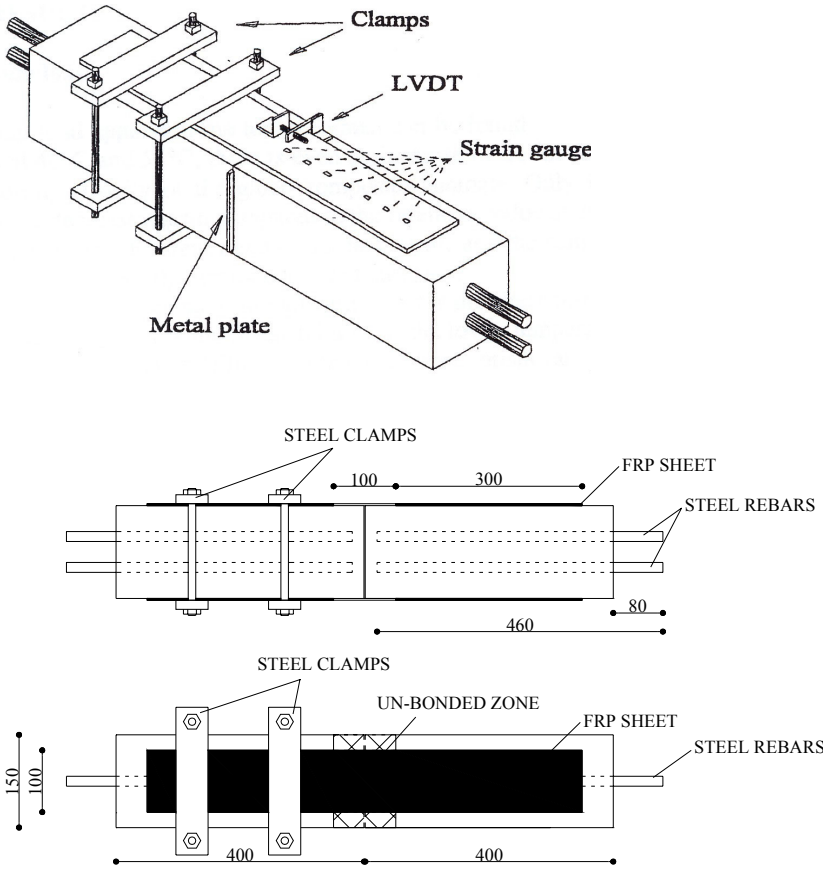

Fig. 1. Test specimen

The FRP reinforcement (100x700 mm) is glue on two opposite sides of the concrete specimen, taking into account the application procedures as provided by the manufacturer. For roughening of the concrete, grinding with a carborundum stone was used. The FRP reinforcement is left un-bonded over a central zone of 100 mm (where the two concrete prisms connect each other). The bonded length equals 300 mm for each prism, which is somewhat higher than the maximum transfer length needed to develop the full anchorage force which can be built up by the FRP-concrete interface. This length has been chosen based on fracture mechanics analysis according to fib Bulletin 14 [7]. On one side of the test specimen, extra fixation of the FRP was provided by means of clamps (Fig. 1), so to force the bond failure at the opposite side.
An overview of the different test specimens and the main test parameters is given in Table 1. As can be noted, bond test have been executed for different temperatures and types of externally bonded FRP (see also next section). The influence of post curing of the adhesive has also been studied by means of two specimens, whereas the specimens were heated for three hours at 110 °C and subsequently cooled at room temperature for three hours. Following, the bond shear test was executed at room temperature.

Test set-up and procedure

A view of the test set-up is given in Fig. 3. The specimens are aligned in an universal testing machine. For the tests at elevated temperature an electrical hollow furnace is used. The oven is placed around the concrete prism without clamps. All gaps between the furnace and the test specimen are filled with mineral wool. The temperature in the furnace is controlled by a thermocouple (type K) that measures the air temperature inside the furnace. The specimen is heated during at least 3 hours before the actual bond shear test, allowing the specimen to reach the preset temperature. Following, the specimen is subjected to a deformation controlled tensile test. The loading rate was taken equal to 0.1 mm/min.
During the bond shear tests the following measurements are performed. The total tensile force applied on the test specimen is recorded by the pressure transducer of the tensile testing machine. The relative displacement between the FRP reinforcement and the concrete was recorded with two displacement transducer, one for both monitored sides. The transducers are fixed to the concrete and directly connected to the FRP reinforcement at the loaded end (at the location of the transition between the central un-bonded and the bonded zone). Electrical strain gauges were used on the FRP reinforcement on both sides, to measure the strains along the bonded length. To verify the temperature influence on the strain gauges, for some of the specimens, a dummy strain gauge glued on a small and unloaded FRP strip was also provided in the oven.

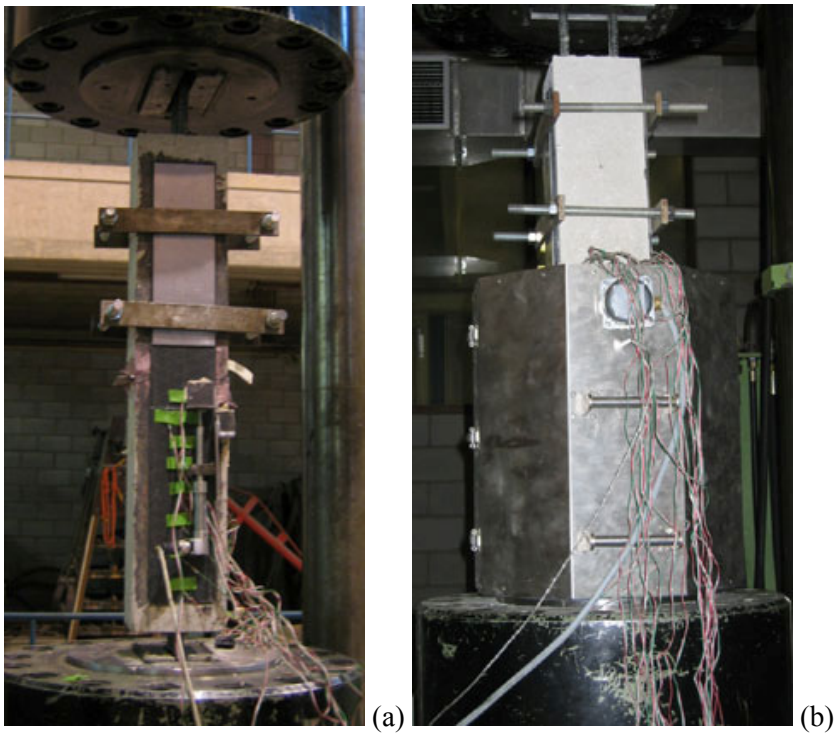
(a) (b)

Fig. 2. View of the test set-up: (a) at room temperature, (b) at elevated temperature

Material properties

The mechanical properties of utilized materials were experimentally evaluated at the age of the testing. The mean concrete compressive strength determined on cubes with side length 150 mm ($f_{c,cub}$) equals 50.3 N/mm², 50.2 N/mm² and 41.3 N/mm² for the three concrete batches respectively. The batch number of the each specimen is given in Table 1. The FRP EBR systems used in this test program and the tensile properties of the FRP reinforcement (nominal thickness t, FRP tensile strength f_f, effective FRP stiffness tE_f) are reported in Table 2.
In this table, also the glass transition temperature T_g as experimentally determined by means of the DSC (Differential Scanning Calorimetry) method is reported. The T_g analysis has been performed at Lecce University on three samples of each epoxy resin. The epoxy samples were cured at room temperature during at least 3 days before testing. The samples were held for 1.0 minute at 5°C and subsequently heated in a nitrogen atmosphere from 5°C to 200°C at 10°C/min. For both epoxy types a T_g of ~ 55°C was found. A similar DSC analysis at Ghent University, which involves also a pre-heating cycle between - 50°C and 200°C (rate 10°C/min), resulted in a T_g of 81°C. Considering T_g equal to 55°C the test temperatures of 50°C, 65°C and 80°C represent -10%, +18% and +45% of the glass transition temperature, respectively.

Tab. 2. Material properties of the FRP EBR

Type	FRP	Epoxy	t (mm)	f_f (N/mm²)	tE_f (kN/mm)	T_g DSC[4] (°C)	T_g DSC[5] (°C)
CFRP sheet	Csheet 240[1]	PC5800[2]	0.117	2600	26.4	55	(not determ.)
CFRP laminate	PC CarboComp[2]	PC5800 BL[2]	1.0	2450	176.0	55	81
GFRP sheet	SyncoTape[3]	PC5800[2]	0.300	780	21.9	55	(not determ.)

By companies [1] S&P, [2] ECC and [3] Syncoglas
DSC method with[5] and without[4] pre-heating cycle

TEST RESULTS

Maximum load and failure aspect

An overview of the obtained mean failure load Q_u, the ratio $Q_u/Q_u(20°C)$ and the failure aspect are given in Table 3. For the C_S specimens and with respect to the reference at 20°C, an increasing ultimate load is observed at 50°C and to a lesser extent at 65°C. A load reduction is found at 80°C for both C_S and G_S specimens, though the extent of the reduction in failure load differs significantly. A similar trend has been observed in [5]. For the C_L specimens and with respect to the reference at 20°C, a load reduction is found at 50°C (however for these specimens the concrete strength is lower) and a load increase at 80°C. This contradicting behaviour for the C_L specimens is unclear. However, eccentricities during loading were observed from the LVDT measurements, which may have influenced the results.
The 'post-cured' specimens (C_L_PC), have been subjected (in an unloaded state) to a temperature cycle up to 110°C before bond testing at 20°C. For these specimens also a reduced ultimate load is found, which appears contradicting with the higher T_g value found for epoxy samples subjected to a pre-heating cycle (Table 2). Because of the apparent inconsistency in test results of the C_L specimens no sound observations can be made for the post cured specimens.
Two different types of failure were observed for the considered tests. Whereas most specimens failed by debonding, also FRP fracture was observed (in combination with debonding) for the specimens with surface bonded CFRP sheet (C_S specimens). The FRP rupture occurred however at loads below the tensile capacity derived from FRP tensile testing. This unexpected type of failure has also been observed by [8] and may relate to both eccentricities in the test configuration and the complex state of stress near ultimate.
The bond failure at 20°C of the specimens with surface bonded FRP sheet is typically characterized by a thin layer of a concrete attached to the FRP reinforcement. The influence of elevated temperature on the bond failure aspect of bonded FRP sheet is illustrated in Fig. 3. At T = 50°C a cohesion failure is observed, with a thin layer of concrete attached to the FRP. Increasing the temperature (i.e. T = 80°C) a debonding at the interface between adhesive and FRP reinforcement occurred (adhesion failure). This observation complies with the strength reduction of the adhesive at high temperature. Failure at T = 65°C was intermediate between cohesion and adhesion failure.
In the case of bonded FRP laminate for all test temperatures, a mixed failure was obtained characterized by cohesion failure, adhesion failure at the epoxy-concrete interface and adhesion failure at the epoxy-FRP

interface. Nevertheless, adhesion failure at the epoxy-FRP interface tends to be predominant at higher temperatures.
This somewhat different behaviour between CFRP sheet (applied by wet lay-up) and CFRP laminate (applied by gluing of the prefab composite strips) may be linked to the different type of epoxy resin and the higher quality of the reinforcement made by industrial technological process

Tab. 3. Test results at ultimate

Specimens	Q_u (kN)	$Q_u/Q_u(20°C)$ (-)	Failure aspect
C_S_20	12	1.00	FF/BF
C_S_50	15	1.25	FF
C_S_65	13	1.08	FF
C_S_80	11	0.92	FF
C_L_20	40	1.00	BF
C_L_50	34	0.85	BF
C_L_80	44	1.10	BF
C_L_PC	34	0.85	BF
G_S_20	15	1.00	BF
G_S_80	12	0.80	BF

BF: bond failure
FF: fracture of FRP reinforcement

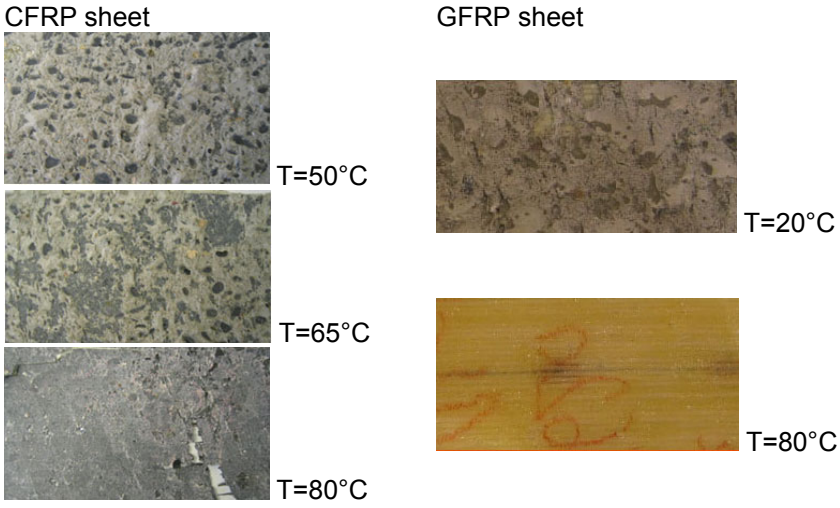

Fig. 3. Bond failure aspect of specimens with surface bonded FRP sheet

Maximum bond stress

Bond stresses are evaluated based on the experimentally recorded strains along the FRP. Referring to two consecutive strain gauges, ranging Δx_i, the equilibrium equation assuming uniform distribution of the bond stress in the analysed discrete interval, gives:

$$\tau(x) = E_f t \frac{\Delta\varepsilon_i}{\Delta x_i} \quad (1)$$

with, $\tau(x)$ the bond stress in the FRP reinforcement between two consecutive strain gauges, E_f and t the modulus of elasticity and the nominal thickness of the FRP reinforcement respectively, and $\Delta\varepsilon_i$ the FRP strain difference between the two considered strain gauges.

To make a more correct comparison of the maximum bond stress between specimens of different concrete batches, a correction coefficient is used based on the relationship between bond strength and compressive concrete strength given in [9]:

$$\sqrt{f_{c,cub} / f_{c,cub,REF}} \quad (2)$$

The maximum bond stress (τ_{max}) for the different test specimens is reported in Table 4. It can be noted that the maximum bond stress at 20°C differs for the 3 types of externally bonded reinforcement and relates to the effective FRP stiffness (tE_f), the quality of the bond interface and the surface texture. Comparing the results at 20°C and 80°C for the different reinforcement types, a significant decrease of the maximum bond stress can be observed for elevated temperatures beyond the glass transition temperature. In particular, τ_{max} decreases with 54% in the case of the CFRP sheet, 72% for the GFRP sheet and 25% for the CFRP laminate. Note that higher temperatures than those used in this test program are needed to have a complete degradation of the bond strength.
Given the temperature dependant properties of the epoxy and the observed failure aspect at 80°C (adhesion failure at epoxy-FRP interface), the decrease in maximum bond stress can be expected. Nevertheless, as the T_g value of the two utilized epoxy resins are both around 55°C, the difference in reduction of maximum bond stress appears not only influenced by the chemical process of the glue at elevated temperature. Likely, the reduction in bond performance has also been affected by the different surface textures and the quality of the bond interface. The latter relates to the application process (which is different for sheets versus laminates) and the quality of the execution, e.g. in terms of fibre alignment, uniform resin distribution, glue thickness and occurrence of micro voids. Hereby, it appears that at elevated temperatures the bond performance is more sensitive to these quality aspects.
Comparing the results at 50°C which is slightly below the glass transition temperature, an increased maximum bond stress is found for CFRP sheet and a decreased value for CFRP laminate. Similar results are reported in the literature [5, 10], though it is not clear to which extent this result is due to test variability (as discussed in the section 'maximum load and failure aspect') or to possible variations in the chemical processes when reaching the T_g value.
In general terms and compared to the behaviour at 20°C, the results preliminarily suggest that the maximum bond stress and anchorage load of the surface bonded FRP (with given anchorage length) first increases with elevated temperature and only decreases for temperatures equal to or beyond the glass transition temperature. The method of determining the glass transition temperature may yield considerable differences in the obtained T_g value. Results obtained here seem to suggest that a T_g value determined based on DCS including a pre-heating cycle at high temperature may overestimate the temperature at which a decrease of the ultimate load is found.

Tab. 4. Main test results

Specimens	Max. bond stress (N/mm^2)	Calculated slip (mm)	Measured slip (mm)
C_S_20	4.2	0.181	0.661
C_S_50	5.6	0.197	0.508
C_S_65	3.7	0.271	0.205
C_S_80	2.0	0.116	0.078
C_L_20	5.6	0.087	0.270
C_L_50	3.3	0.183	0.169
C_L_80	4.2	0.237	0.866
G_S_20	3.4	0.186	0.645
G_S_80	1.0	0.182	0.221

Strain distribution and bond stress-slip relation

The bond behaviour along the bond length is reflected by the strain readings at different load levels. A comparison of the strain along the FRP reinforcement for the different reinforcement types is reported in Fig.4 at a load level of 4 kN and for the tests at 80°C. At this stage the specimen G_S_80_a is at 50% of its ultimate load, while C_L_80_a and C_S_80_b are at 9% Q_u and 32% Q_u, respectively. The strain curves along the bond length show the influence of the stiffness on the strain distribution. Both S_80 specimens

have a fairly comparable strain distribution, while the L_80 specimen is characterized by much lower strain, hence stiffer behaviour. This corresponds with the effective stiffness (Table 2) of the three types of bonded reinforcement. Similar results were found for all tested specimens.
Given the strain distribution, the slip between FRP reinforcement and concrete can been calculated through integration of the strain along the bonded length and hence the bond stress-slip relationship can be derived. As the bond length is longer than the maximum bond length by [7], the slip at the free end can be neglected. Also neglecting the concrete strain, the slip is obtained as:

$$s = \sum_{i=1}^{n} \varepsilon_i \Delta x_i \tag{3}$$

with, n the number of strain measurements along the bond length, ε_i the FRP strain at the measured location and whereas the origin of the x axis is taken at the loaded end.
The measured and calculated slip at the loaded end are given in Table 4. Both slip measurements (direct and indirect by calculation from strain measurements) differ to a large extent, which relates to the technically difficult constraints of direct slip measurements. In this test programme, the obtained experimental slip measurements are rather used to evaluate the relative behaviour of the different specimens and the occurrence of possible eccentricities in loading. Therefore, in absolute terms, the slip values obtained from the experimental strain measurements are considered. Increasing the test temperature generally results in an increase of the slip as well. This observation is more pronounced for the specimens reinforced with CFRP laminate than for hand lay-up CFRP and GFRP sheet.
The bond stress-slip (τ-s) behaviour, calculated from the strain measurements according to equations (1) and (3), is given in Figures 5 and 6. The influence of the type of reinforcement is reported in Fig. 5. From this figure it can be noted that the slope of the ascending branch of the τ-s curves increases with the effective reinforcement stiffness and that the slope for the CFRP and GFRP sheet (with almost the same effective stiffness) are very close. A comparison between the τ-s curves at different test temperature is given in Fig. 6, for the C_L specimens. It can be observed that increasing the temperature results in a less stiff behaviour of the FRP reinforcement - concrete interface.

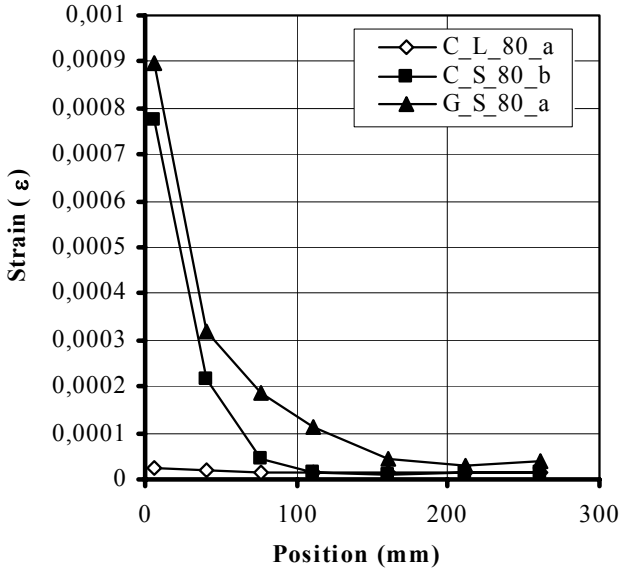

Fig. 4. Strain distribution along the bond length (load level 4 kN, T = 80°C)

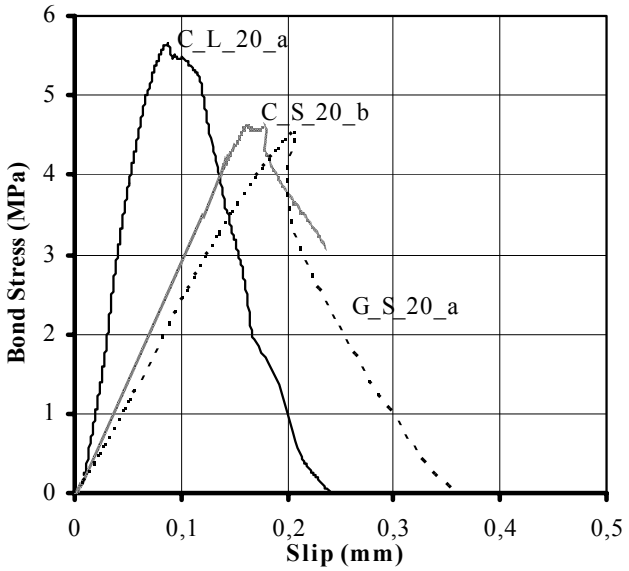

Fig. 5. Bond stress-slip behaviour at T = 20°C

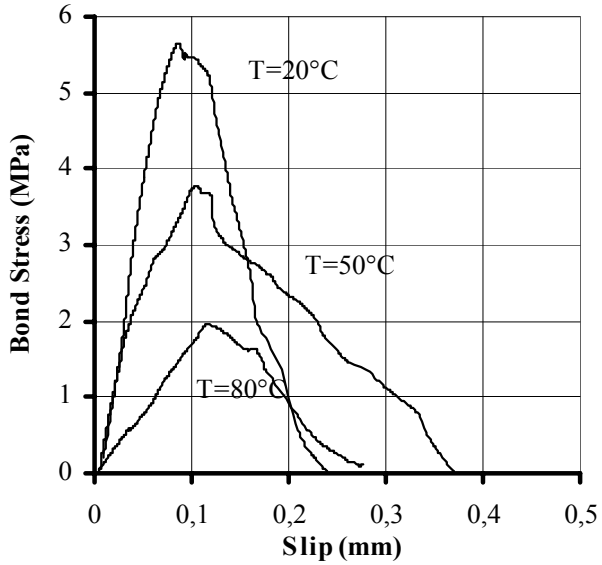

Fig. 6. Bond stress-slip behaviour at different temperatures (for specimens C_L)

Transfer length

Fig. 7 shows the change in bond stress as a function of the relative load level Q/Q_u, for 3 different regions along the bond length of specimen G_S_20_b. In this figure, the bond stress is calculated per region based on the recorded load-strain behaviour of two consecutive strain gauges. For increasing load the bond stress in the region near the loaded end (curve 6-41 mm in the Fig. 7) reaches a peak at about 75% of the maximum load and then starts to decrease fairly abrupt. At the same time the bond stress in the adjacent region (curve 41-76mm) starts to increase. This observation clearly demonstrates initiation of debonding at the loaded end, along with load transfer further along bond length. This phenomenon is observed progressively from one region to another until complete debonding failure [11].
In the Fig. 8 the strain versus position (starting from the loaded end) along the bond length is given for different load levels. Also from this figure, the load transfer mechanism can be observed. For moderate load levels, when load transfer further along the bond length has not yet initiated, the strain distribution profile is characterized by an exponentially descending branch. The distance required for the strain to reach almost zero is defined as the initial transfer length (L_{ti}). At higher load levels, the transfer region gradually extends towards the unloaded end.

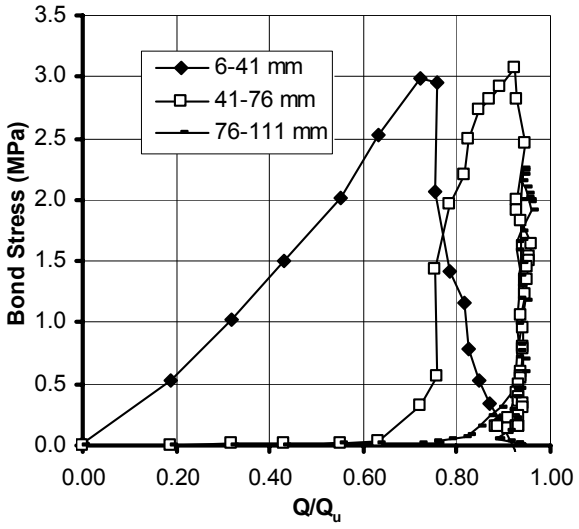

Fig. 7. Bond stress as function of relative load level (G_S_20_b)

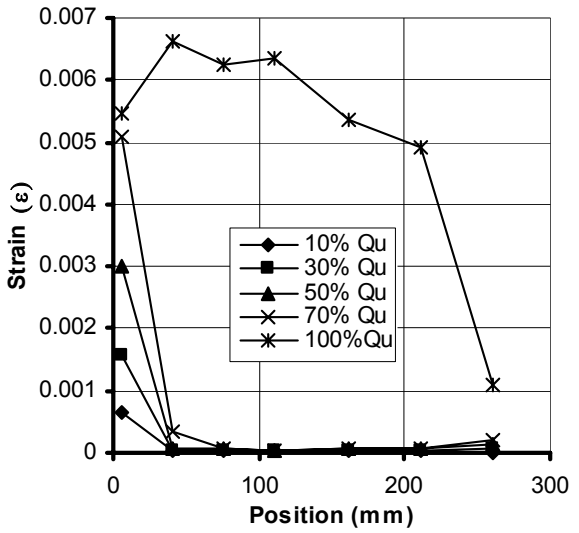

Fig. 8. Strain versus position along bond length (G_S_20_b)

The initial transfer length was evaluated for the different specimens and is reported in Table 5. It can be noted that for all types of tested FRP reinforcement, the initial transfer length increases with the test temperature. Comparing the initial transfer length at 20°C and 80°C, a difference by a factor 2.5 to 3.0 is found. This result appears particularly interesting because the apparent increase of the maximum anchorage load with respect to elevated service temperatures below T_g seems to link to a considerable increase of the initial transfer length.

Tab. 5. Initial transfer length

Specimens	L_{ti} (mm)	$L_{ti}/L_{ti}(20°C)$ (-)
C_S_20	40	1.00
C_S_50	41	1.02
C_S_65	108	2.70
C_S_80	104	2.60
C_L_20	100	1.00
C_L_50	153	1.53
C_L_80	251	2.51
G_S_20	68	1.00
G_S_80	215	3.16

CONCLUSIONS

The results obtained for the test programme discussed in this paper demonstrate that the bond performance, in terms of bond stress, slip and stiffness, is significantly influenced by the service temperature. As a consequence the occurrence of elevated service temperature must be taken into account from a design point of view.
The results preliminarily suggest that the anchorage load of the surface bonded FRP (with given anchorage length) first increases with elevated temperature and only decreases for temperatures equal to or beyond the glass transition temperature. For the considered tests at 80°C (about $1.5T_g$), the maximum bond stress decreased by 54% in the case of CFRP sheet, 72% for GFRP sheet and 25% for CFRP laminate.
With increasing temperature:

- the maximum bond stress generally increases (though this observation was not obtained for all specimens) and decreases only for temperatures equal to or above the glass transition temperature,
- the bond interface is characterized by a less stiff behaviour (slope of the ascending branch of the τ-s curves),
- the initial transfer length (this is the bond transfer length in the loading stage before load transfer further along the bond length occurs) increases up to a factor 2.5 to 3.0 at 80°C,
- the bond performance may become more sensitive to bond quality aspects such as fibre alignment, micro voids in the glue, etc.
- more and more an adhesion failure at the interface is observed: meaning that at temperatures similar to or higher than the T_g, the strength of the adhesive drops below that of the concrete causing bond failure at the FRP-epoxy interface.

For the temperature range tested in this programme (till about 1.5 T_g – glass transition temperature determined without preheating cycle), no complete degradation of the bond strength was found.
The method of determining the glass transition temperature may yield considerable differences in the obtained T_g value. Results obtained here seem to suggest that a T_g value determined based on DCS (Differential Scanning Calorimetry) including a pre-heating cycle at high temperature may overestimate the temperature at which a decrease of bond properties is found for the case of FRP cured at ambient conditions.
With respect to the different types of FRP it was found that the effective stiffness (tE_f) of the surface bonded FRP is an important parameter.

REFERENCES

1. Matthys S, Taerwe L. FRP reinforcement: developments in Europe, *Concrete*, The Concrete Society, 2001; 35 (6):20-21.
2. Blontrock H., Taerwe L., Matthys S. Properties of fiber reinforced plastics at elevated temperatures with regard to fire resistance of reinforced concrete members, *4th International Symposium on Fiber Reinforced Polymer Reinforcement for Reinforced Concrete Structures (FRPRCS-4),* ACI International SP-188, ed. Dolan CD, Rizkalla S, Nanni A, Baltimore, October-November 1999, 43-54.

3. Blontrock H, Taerwe L, Vandevelde P. Fire testing of concrete slabs strengthened with fibre composite laminates, *Proceedings of the fifth Int. Conf. on Fibre Reinforced Plastics for Reinforced Concrete Structures (FRPRCS-5)*, Volume 1, ed. by Burgoyne CJ, Cambridge, July 2001, 547-556.
4. Blontrock H. Analyse and modelling of the fire resistance of concrete elements with externally bonded FRP reinforcement (in Dutch), *PhD thesis*, Ghent University, 2003.
5. Blontrock H, Taerwe L, Vanwalleghem H. Bond testing of externally glued FRP laminates at elevated temperature*, Proceeding of the International Conference on Bond in concrete- from research to standard*, Budapest, Hungary, 2002, 648-654.
6. Aiello MA, Frigione M, Leone M, Aniskevich AN, Plushchik OA. Effect of temperature on mechanical performances of CFRP rebars, *Proceeding of the 24th International SAMPE Europe Conference of the Society for the Advancement of Material and Process Engineering*, Paris, France, 2003, 239-249.
7. fib. Externally bonded FRP reinforcement for RC structures, fib Bulletin 14, *Technical report on the Design and use of externally bonded fibre reinforced polymer reinforcement (FRP EBR) for reinforced concrete structures*, Working Party EBR of Task Group 9.3 'FRP reinforcement for concrete structures', International federation for structural concrete, Lausanne, 2001.
8. Brosens K. Anchorage of externally bonded steel plates and CFRP laminates for the strengthening of concrete structures, *PhD Thesis*, Katholieke Universiteit Leuven, 2001.
9. CEB-FIP. *CEB-FIP model code 1990*, Comité Euro-International du Béton, Lausanne, Switzerland, 1991.
10. Galati N, Nanni A, Dharani LR, Focacci F, Aiello M. Thermal effects on bond between FRP rebars and concrete, *Construction and Building Material*, in print.
11. Bizindavyi L, Neale KW. Transfer length and bond strength for composites bonded to concrete, *Journal of composites for construction*, ASCE, November 1999: 153-160.